RERTR 2010 — 32nd INTERNATIONAL MEETING ON
REDUCED ENRICHMENT FOR RESEARCH AND TEST REACTORS

October 10-14, 2010
SANA Lisboa Hotel
Lisbon, Portugal

THERMAL-HYDRAULIC SAFETY ANALYSES FOR CONVERSION OF THE LAUE LANGEVIN INSTITUTE (ILL) HIGH FLUX REACTOR (RHF) FROM HEU TO LEU FUEL

A. Tentner[1], F. Thomas[2], A. Bergeron[1], J. Stevens[1]

1. Argonne National Laboratory, Argonne, Illinois, USA
2. Institut Laue-Langevin, Grenoble, France

ABSTRACT

This paper presents the results of thermal-hydraulic safety analyses for conversion of the High Flux Reactor (RHF) from the use of HEU fuel to the use of UMo LEU fuel. The objective of this work was to show that is feasible, under a set of manufacturing assumptions, to design a new RHF fuel element that could safely replace the HEU element currently used. The new proposed design has been developed to maximize performance, minimize changes and preserve strong safety margins.

Thermal-hydraulic models of the RHF with HEU fuel have been developed independently at ANL using the CFD code STAR-CD and at ILL using the CFD code CFX. These models were qualified by comparing the results of analyses with RHF Safety Analysis Report data. The thermal-hydraulic model STAR-CD was then used to evaluate the RHF performance for the proposed LEU fuel element. The results of these analyses show that the thermal-hydraulic margins for the proposed LEU design may be slightly reduced compared to HEU but still satisfy technical specifications.

Introduction

The High Flux Reactor (RHF) of the Laue Langevin Institute (ILL) based in Grenoble, France is a research reactor designed primarily for neutron beam experiments for fundamental science. It delivers one of the most intense neutron fluxes worldwide, with an unperturbed thermal neutron flux in the reflector of $1.5x10^{15}$ n/cm^2/s. The reactor has been conceived to operate at a nuclear power of 57 MW but currently operates at 52 MW. The reactor currently uses a Highly Enriched Uranium (HEU) fuel.

In the framework of its current non-proliferation policies, the international community aims to minimize the amount of available nuclear material that could be used for nuclear weapons. In this geopolitical context, most worldwide research and test reactors have already started a program of conversion to the use of Low Enriched Uranium (LEU) fuel. A new type of LEU fuel based on a mixture of uranium and molybdenum (UMo) is expected to allow the conversion of compact high performance reactors like the RHF.

This paper presents preliminary results of reactor thermal-hydraulic performance and steady state safety analyses for conversion of the RHF from the use of HEU fuel to the use of UMo LEU fuel. The objective of this work was to show that is feasible, under a set of manufacturing assumptions, to design a new RHF fuel element that could safely replace the HEU element currently used. The new proposed design has been developed to maximize performance, minimize changes and preserve strong safety margins.

Neutronics and thermal-hydraulics models of the RHF have been developed and qualified by benchmark against experiments and/or against other codes and models. The models developed were then used to evaluate the RHF performance if LEU UMo were to replace the current HEU fuel "meat" without any geometric change to the fuel plates. Results of these direct replacement analyses have shown a significant degradation of the RHF performance, in terms of both neutron flux and cycle length.

Consequently, ANL and ILL have collaborated to investigate alternative designs. A promising candidate design has been selected and studied, where the total amount of fuel is increased, without changing the external plate dimensions, by relocating the burnable poison. In this design the required fuel element changes are reasonably small. With this new LEU design, neutronics analyses presented in a companion paper have shown that the RHF performance could be maintained at a high level: 2 day decrease of cycle length (to 47.5 days at 58.3 MW) and 1-2% decrease of brightness in the cold and hot sources in comparison to the current typical operation. Thermal-hydraulic studies described in this paper show that the thermal-hydraulic and shutdown margins for the proposed LEU design would satisfy technical specifications.

1. Review of RHF Geometry

The RHF has one fuel element, made of 280 curved plates welded to two concentric aluminum tubes. All of the curved plates are bent into an involute shape. This shape has the advantage of maintaining a constant distance between two plates within the overall cylindrical geometry of the compact core. Figure 1 is a diagram of the fuel element. The element is placed

in a heavy water tank which is itself surrounded by a light water pool. The heavy water plays the dual role of neutron moderator and coolant. The RHF is controlled by a central rod. The position of the control rod is adjusted during the cycle to maintain criticality. For the current HEU fuel, two borated zones exist in the lower and upper parts of each fuel plate. The borated zones help to reduce power peak intensities at the axial edges of the plates. The HEU fuel is a mix of U-Al_x in an aluminum matrix. The enrichment in ^{235}U is 93%.

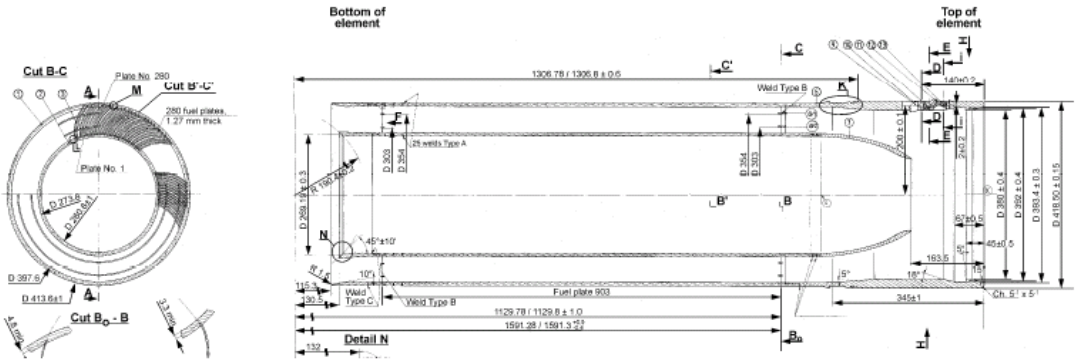

Figure 1: Fuel element overview [Ref. 1]

The dimensions of the HEU fuel plate including the fuel meat, the borated zones and the cladding are illustrated in Figure 2. The coolant enters at the top of the fuel element, flows downward, and exits at the bottom.

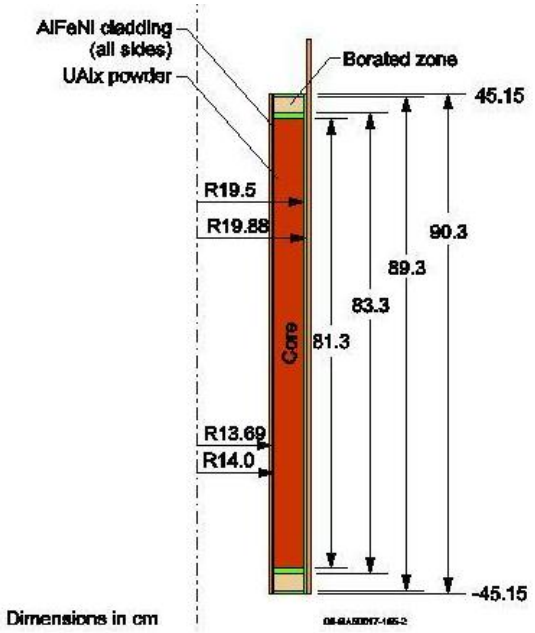

Figure 2: HEU fuel plate dimensions [Ref. 2]

2. The CFD Models of the HEU and Proposed LEU RHF Reactor

The thermal-hydraulic performance of the RHF has been evaluated using two independent models: one model, developed at ANL, is based on the STAR-CD CFD code [Ref. 3], the other model, developed at ILL, is based on the CFX CFD code [Ref. 4]. These models are described below.

2.1 The CFD Models of the HEU RHF Reactor

The STAR-CD model of the RHF describes two coolant channels bound by a full fuel plate, two half-plates and the outer and inner rings, as illustrated in Figure 3a. The outer surfaces of the two half-plates are designated as cyclic boundaries. The fuel plate is constructed as an arc of a circle, with the radius of the inner cladding surface $R_{cladding}$ = 85.3 mm. This is an approximation of the involute and was selected because the same approximation is used in the neutronic calculations that determine the RHF power generation distribution. The CFD model is script-based and thus the geometry, mesh size and physical parameters can be easily modified for future sensitivity studies.

The CFX model, shown in Figure 3b, describes only one coolant channel bound by two fuel half-plates and the outer and inner rings. The fuel half-plates and the coolant are involutes of a circle with a radius of 136.81 mm. The outer ring region is a simple extension of the involutes whereas the inner ring is a -y straight line extension of the geometry.

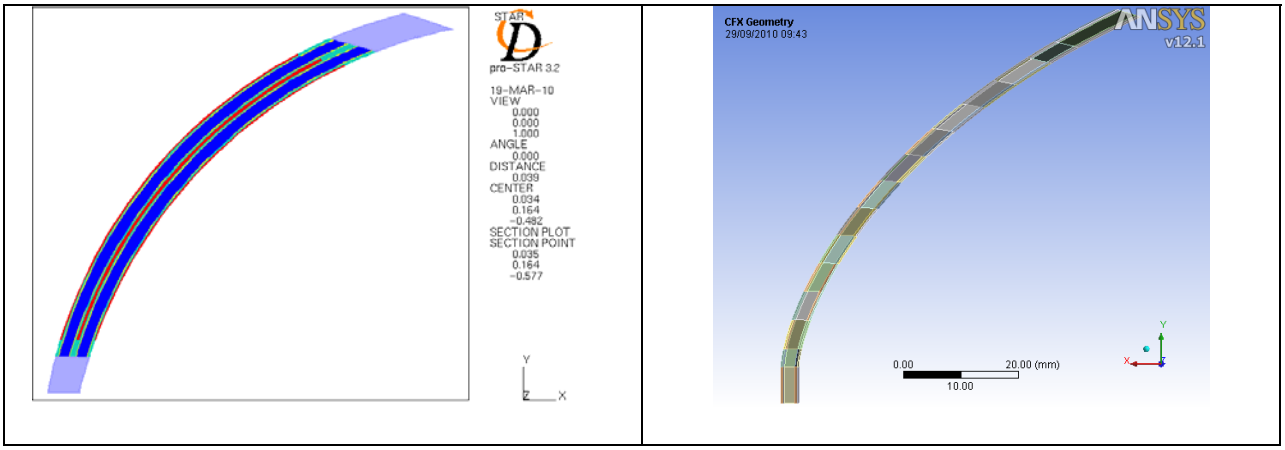

Figure 3: Cross section through the coolant channel and fuel plates, viewed from the +z direction: a) Left: STAR-CD model. Blue - coolant; red - fuel; green - cladding; yellow - cladding surface cells; light blue - inner and outer rings, and b) Right: CFX Model. The fuel meat region is divided into 11 radial zones corresponding to those used in the neutronic calculations.

The axial structure of the STAR-CD CFD model of the HEU configuration is illustrated in Figure 4. The model includes the cladding, borated regions and fuel meat region, with the dimensions shown in Figures 1 and 2. A short inlet plenum with L = 1 cm was added at the inlet. A longer outlet plenum is used at the outlet, with L = 5 cm. Both plena are needed to ensure convergence of the pressure solution in the presence of parallel coolant channels. The longer outlet plenum is necessary due to the presence of the expansion at the exit of the inter-plate sub-channels, which can cause numerical problems at the outlet boundary condition if this boundary is too close to the flow expansion. The CFX HEU model has a similar axial structure but, as the CFX model is a single channel model, no plena were included.

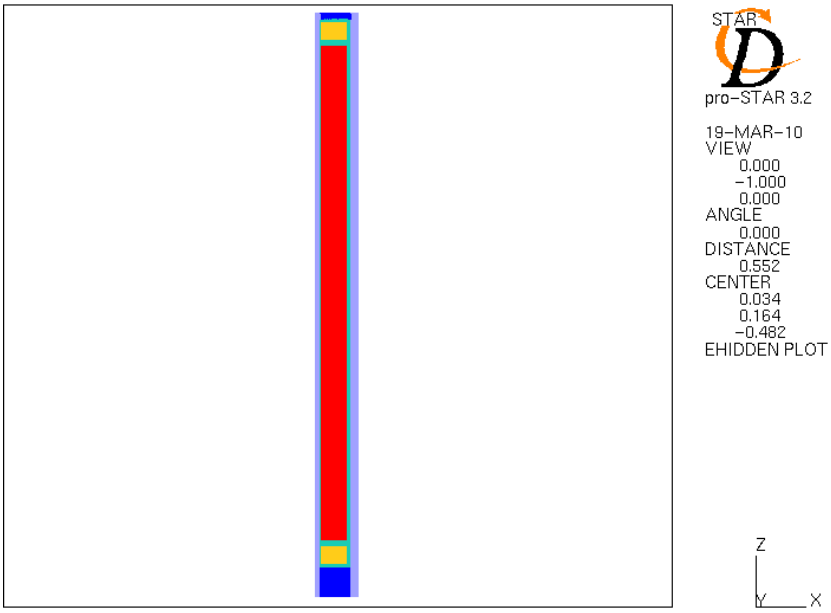

Figure 4: Cross section through the centerline of the HEU fuel plate, viewed from the -y direction illustrating the features of the CFD STAR-CD model: blue - coolant; red - fuel meat; green - cladding; orange - borated regions; light blue - inner and outer rings

2.2 The CFD Model of the Proposed LEU Reactor

The LEU RHF fuel element uses a fuel plate with the same overall dimensions and shape as the HEU RHF fuel element, but the boron regions at the top and bottom of the fuel plate have been removed and the fuel meat region has been extended axially. The boron region is now located outside the region modeled by the CFD model. Its influence on the thermal-hydraulics is taken into account through the power distribution provided to the CFD model by the neutronic calculations. The geometry of the LEU CFD is illustrated in Figure 5. The fuel meat region now extends from 5 mm below the top of the plate to 5 mm above the bottom of the plate, for a total length of 893 mm covering the axial length occupied in the HEU fuel plate by the boron regions, fuel meat and separating cladding regions shown previously in Figure 4. All other geometric features of the CFD models remained the same as described above in Section 2.1.

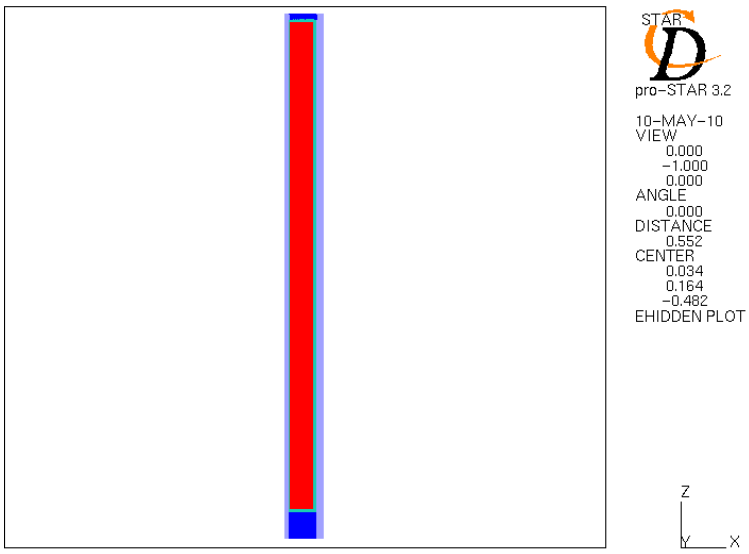

Figure 5: Cross section through the centerline of the LEU fuel plate, viewed from the -y direction illustrating the features of the STAR-CD CFD model: blue - coolant; red - fuel meat; green - cladding; light blue - inner and outer rings

2.3 Turbulence Models and Mesh Sensitivity

The results presented in this paper were obtained using the k-ε turbulence model for both the STAR-CD and CFX models. The k-ε turbulence model uses scalable wall functions and works with y^+ values between 30 and 300, where y^+ is the non-dimensional wall distance. The STAR-CD model y^+ values were around 30, while the corresponding values for the CFX model were about 40. Sensitivity studies were performed with both codes, evaluating the changes in the maximum coolant wall temperature due to changes in the y^+ values. The results obtained with both models show that, as expected, the maximum coolant temperature at the cladding surface increases only slightly, less than 1 K, when the y^+ value is decreased from 60 to 30.

We also used the CFX model to check the relevance of the turbulence model, by using the k-ω turbulence model in exploratory calculations. The k-ω turbulence model is valid for low y^+, typically less than 10. Results obtained with the CFX model using the k-ω turbulence model with $y^+ = 4$ lead to maximum coolant wall temperatures that are lower by approximately 6 K than the corresponding value obtained with the k-ε turbulence model described above. Decreasing y^+ values increases the number of elements in the mesh. For the present study, we have less than 5×10^5 elements for $y^+ = 40$, but more than 10^7 elements for $y^+ = 4$. Increasing the mesh size increases the calculation time accordingly. The effect of the turbulence model on results will be explored further in future work.

3. CFD Analyses of the HEU and Proposed LEU RHF Reactor

The thermal-hydraulic performance and safety margins of the RHF with LEU and HEU have been evaluated for nominal conditions and two cases selected in the safety report [Ref. 5]. The results obtained for nominal operating conditions are presented in the following sections.

3.1 Boundary Conditions

The inlet boundary is located at the entrance of the upper plenum, with the coolant flowing downwards and the outlet located at the bottom of the lower plenum. The inlet coolant volumetric flow rate is Q = 2372 m^3/hr (2329 m^3/hr in the CFX model) and the inlet coolant temperature is 30 C. The coolant outlet pressure is 4.36 bar absolute (4 bar absolute in the CFX model).

In the STAR-CD model, the inner ring wall boundary temperature was 30 C and the heat transfer coefficient at this boundary was 2178 W/m^2/K. The outer ring wall boundary temperature was 50 C and the heat transfer coefficient at this boundary was 1141 W/m^2/K.

In the CFX model, the inner ring wall boundary was assumed adiabatic. For the outer ring wall boundary condition, a heat transfer coefficient of 1000 W/m^2/K was chosen, with an outside temperature of 30 C.

3.2 Power Source

The power source distribution in the LEU fuel meat was provided by separate neutronic calculations for a mesh with 179 cells in the axial direction (178 cells with a length of 0.5 cm and one cell with the length of 0.3 cm), 11 cells in the plate “radial” direction (i.e., from inner edge of fuel meat to outer edge of fuel meat) and one cell covering the thickness of the fuel meat. A procedure was developed to remap the neutronic distribution on the STAR-CD CFD fuel meat mesh described above, with 60 axial cells, 30 cells in the plate “radial” direction and 4 cells across the fuel meat thickness. This procedure ensures that the total power used in the CFD analysis is the same as the total power predicted by the neutronic calculations. Neutronic calculations predict that the total RHF power generated in the LEU fuel meat is 54.39 MW for a core producing 57 MW nuclear. This power was increased in the STAR-CD CFD calculations described in this section to 55.06 MW, in order to account for the additional power generated in the coolant and structures. In the STAR-CD CFD calculations all of the 55.06 MW was assumed to be generated in the fuel meat. In the LEU CFX model 54.07 MW are generated in the fuel meat, 0.41 MW in the heavy water, 0.35 MW in the cladding and 0.24 MW in the inner and outer rings. The total thermal power is therefore 55.1 MW.

A similar procedure was used for HEU analyses described below. The total power modeled in the HEU analysis was 53.6 MW for a core producing 57 MW nuclear, in order to be consistent with the existing SAR. That power breakdown was described in the SAR as 53.0 MW generated in the fuel meat and 0.6 MW generated in the coolant and structures. In the STAR-CD CFD calculations all the 53.6 MW was assumed to be generated in the fuel meat. In the HEU CFX model, 53.39 MW are generated in the fuel meat, 0.41 MW in the heavy water, 0.36 MW in

the cladding and 0.24 MW in the inner and outer rings. The total thermal power is therefore 54.4 MW.

The axial power distributions used by the STAR-CD model for the LEU Relocated Poison Configuration and HEU fuel plates, at the outermost radial cell are shown in Figure 6. The axial power distributions used by the CFX model are similar to those shown in Figure 6, and differ only by a small factor due to the allocation of power generated outside the fuel meat, as explained above.

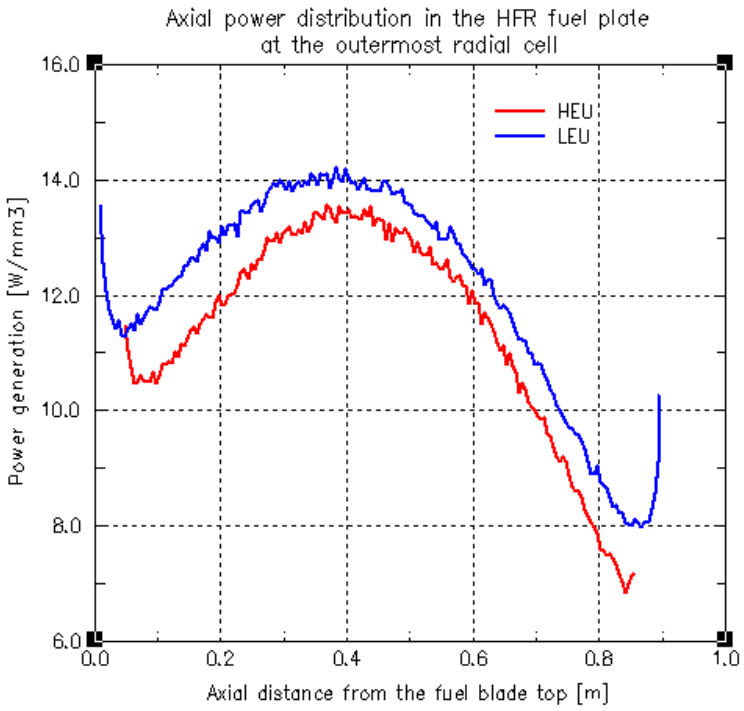

Figure 6: Axial power distribution in the LEU Relocated Poison Configuration and the HEU fuel meat at the outermost radial cell

3.3 Coolant and Cladding Temperature Results

In this section we present the results of CFD LEU calculations performed with the models described in the preceding sections. These results are compared with corresponding results obtained from the HEU calculations. Both the LEU and HEU analyses were performed using the nominal conditions described above in Section 3. The results presented include: a) the maximum coolant cell temperature, which occurs at the center of a coolant cell adjacent to the cladding, b) the maximum coolant temperature at the cladding surface, and c) the maximum cladding surface cell temperature. The best measure of the coolant maximum temperature is provided by the coolant temperature at the cladding surface T(coolant, wall surface), and we use this temperature to determine the margin to coolant boiling in Section 4.

The calculated LEU maximum temperatures are compared with the corresponding HEU temperatures in Table 1. The LEU maximum coolant wall surface temperature is 2.56 C higher than the corresponding HEU temperature.

Table 1: Comparison of LEU and HEU coolant and cladding surface temperatures

	HEU		LEU	
	STAR-CD	CFX	STAR-CD	CFX
T(coolant cell, max) [K]	339.20	337.30	343.20	340.60
T(coolant, wall surface, max) [K]	376.55	368.20	379.11	369.50
T(cladding surface cell, max) [K]	377.50	368.20	380.00	369.50

The axial variation of the coolant temperature at the cladding surface at the radial location of the maximum temperature is shown for the LEU Relocated Poison Configuration and the HEU fuel plates in Figure 7. This figure also includes the corresponding saturation temperature, determined by the local coolant pressure. The difference between the saturation temperature and the coolant wall temperature determines the margin to saturation, which is discussed below in Section 4. The STAR-CD model results shown in Figure 7a indicate that the maximum wall surface temperature occurs for the LEU fuel plate at z = -0.59 m from the top of the plate, at a radial location R = 19.175 cm. For the HEU, the location of the maximum surface temperature is at z = -0.525 m from the top of the plate and at the same radial location. For both LEU and HEU the maximum occurs on the outer side of the curved fuel plate (relative to the center of curvature). However, a similar local maximum temperature occurs on the inner side of the plate, which is only 0.1 C lower.

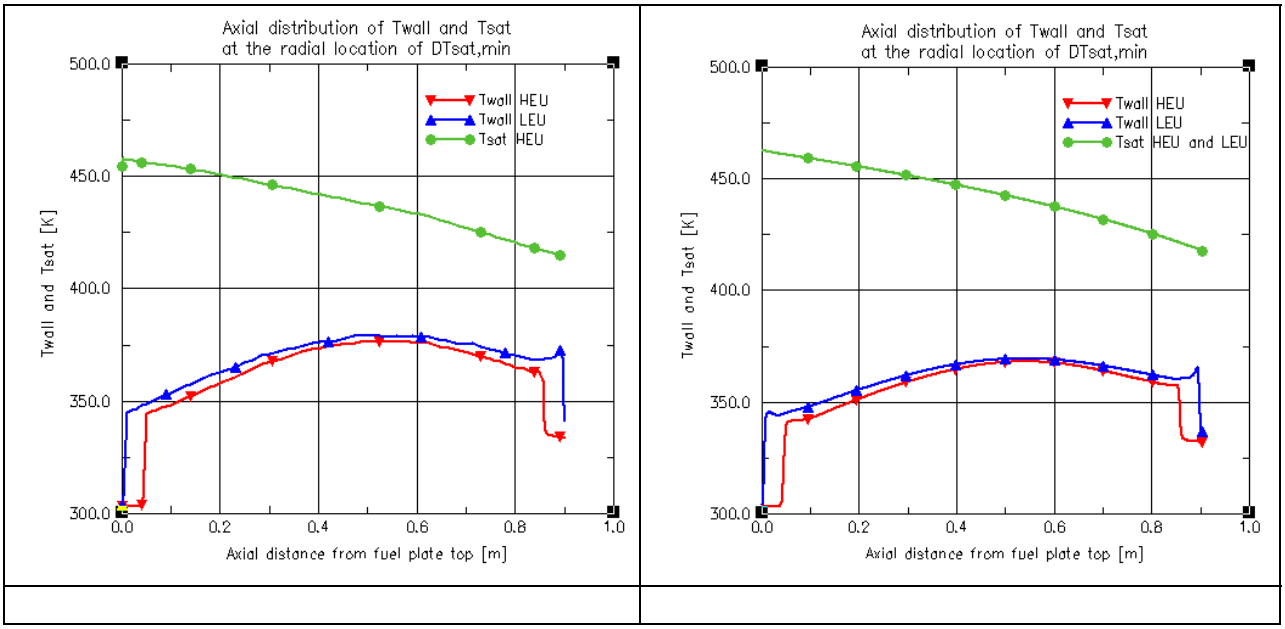

Figure 7: Axial distribution of the coolant temperature at the cladding surface and the saturation temperature at the radial location of DTsat, min for the HEU and LEU fuel plates: a) Left: STAR-CD model results, and b) Right: CFX model results

The CFX model results shown in Figure 7b indicate that the maximum wall surface temperature occurs for the LEU fuel plate at z = -0.59 m from the top of the plate, at a radial location R = 19.2 cm. For the HEU, the location of the maximum surface temperature is at z = -0.525 m from the top of the plate and at the same radial location. The spatial distribution of the coolant temperature at the cladding surface calculated by the CFX model is illustrated for the HEU and LEU fuel plates in figures 8a and 8b, respectively. Similar temperature distributions are obtained with the STAR-CD model.

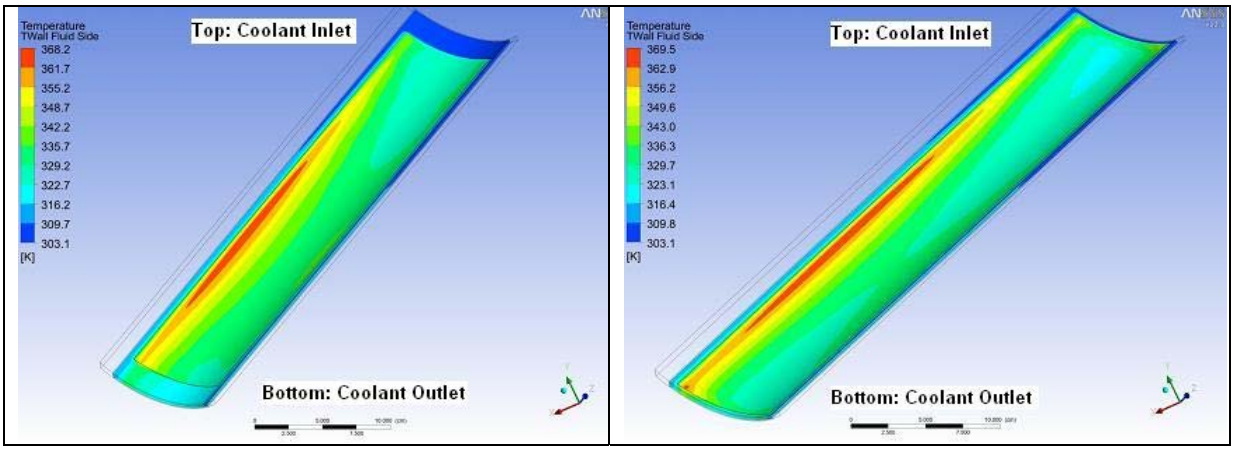

Figure 8: Heavy Water Temperature at the cladding surface: a) Left: HEU fuel plate, and b) Right: LEU fuel plate

The CFX calculations exhibit a lower maximum for the wall temperature than the STAR-CD calculations, the difference being 8.35 K for the HEU and 9.61 K for the LEU fuel plate. Recent calculations performed with a STAR-CD model of the HEU fuel plate using the involute shape show that approximately 5.3 K of the difference is due to the geometrical differences in the current models. The remaining 3 K difference is likely due to several other differences in the model such as different assumptions about the power generation in the coolant and structures, boundary conditions, mesh differences, etc. These differences will be examined in future analyses. The axial location of the maximum coolant wall temperature is the same in both models.

3.4 Predictions of Margin to Boiling

The coolant margin to saturation, onset of nucleate boiling (ONB), and fully developed nucleate boiling (FNB) have been examined for the LEU fuel configuration and compared with the corresponding margins for the HEU fuel configuration. The results obtained with the STAR-CD model were deemed more conservative and are presented below.

3.4.1 Margin to Boiling Results obtained with the STAR-CD CFD model

To determine the minimum margin to saturation DTsat, we conducted a global search over all the coolant cells adjacent to the cladding surface. For each cell the local coolant pressure was used to determine the corresponding D2O saturation temperature Tsat and the margin to saturation was calculated as:

DTsat = Tsat - Tcoolant, wall surface (1)

A similar procedure was used to determine the minimum DTonb, the margin to ONB, and the minimum DTfnb, the margin to FNB:

DTonb = Tonb - Tcoolant, wall surface (2)

DTfnb = Tfnb - Tcoolant, wall surface (3)

where Tonb and Tfnb are the onset of nucleate boiling and full nucleate boiling temperatures and are calculated as:

Tonb = Tsat + DTsuperheat, onb (4)

Tfnb = Tsat + DTsuperheat, fnb (5)

The value of DTsuperheat, fnb was calculated using an established nucleate boiling wall superheat correlation, the Jens-Lottes correlation [Ref. 6]. The wall superheat according to the Jens-Lottes correlation, DTsuperheat, jl is calculated as:

$$DT_{superheat,\,jl} = 0.79\frac{q''^{0.25}}{\exp(\frac{P}{6.2})} \quad (6)$$

where:

q'' = heat flux [W/m2]
P = pressure [MPa]
DT = superheat temperature difference [C]

The Jens-Lottes correlation has been developed for high pressure boiling heat transfer and its applicability to the RHF conditions and CFD RHF analyses should be further investigated.

The value of DTsuperheat, onb was calculated using the widely used Bergles-Rohsenow correlation [Ref. 7]. The ONB superheat according to the Bergles-Rohsenow correlation, DTsuperheat, br is calculated as:

$$DT_{superheat,br} = 0.556\left(\frac{q''}{1082P^{1.156}}\right)^{0.463P^{0.0234}} \quad (7)$$

where:

q'' = heat flux [W/m2]
P = pressure [bar]
DT = superheat temperature difference [C]

The Bergles-Rohsenow correlation was obtained for water over the pressure range 1-138 bar, which includes the RHF operating pressure range. We present below the HEU and LEU results for both correlations. When calculating the local DT superheat with equations (6) or (7), the local heat flux and coolant pressure was used for each coolant cell adjacent to the cladding surface.

The axial variation of the margin to saturation for the HEU and LEU fuel plates is shown in Figure 9.

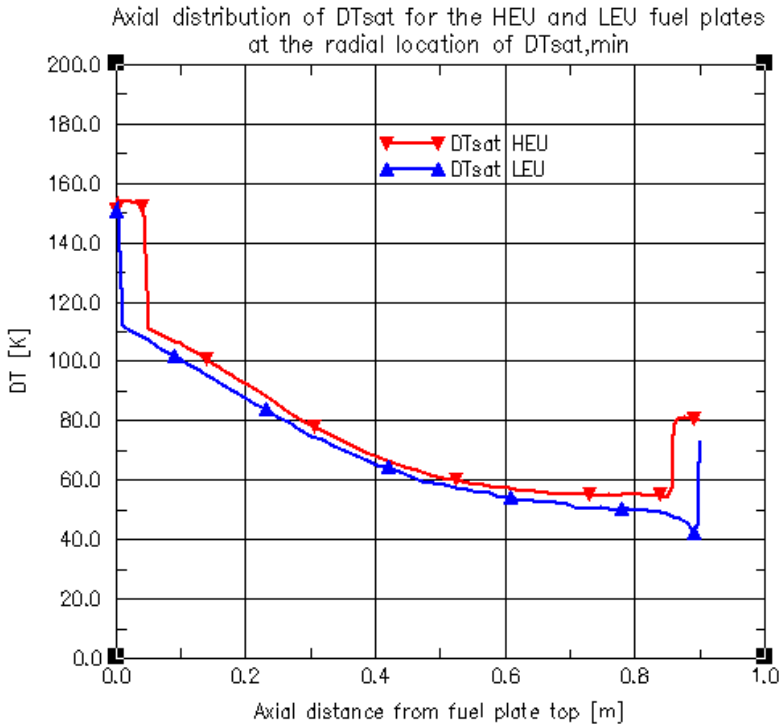

Figure 9: Axial distribution of DTsat for the HEU and LEU fuel plates

The axial variation of the margins to saturation, FNB, and ONB, at the radial location of the global minimum margin to saturation is illustrated in Figure 10a for the HEU fuel plate. The corresponding curves for the LEU plate are shown in Figure 10b.

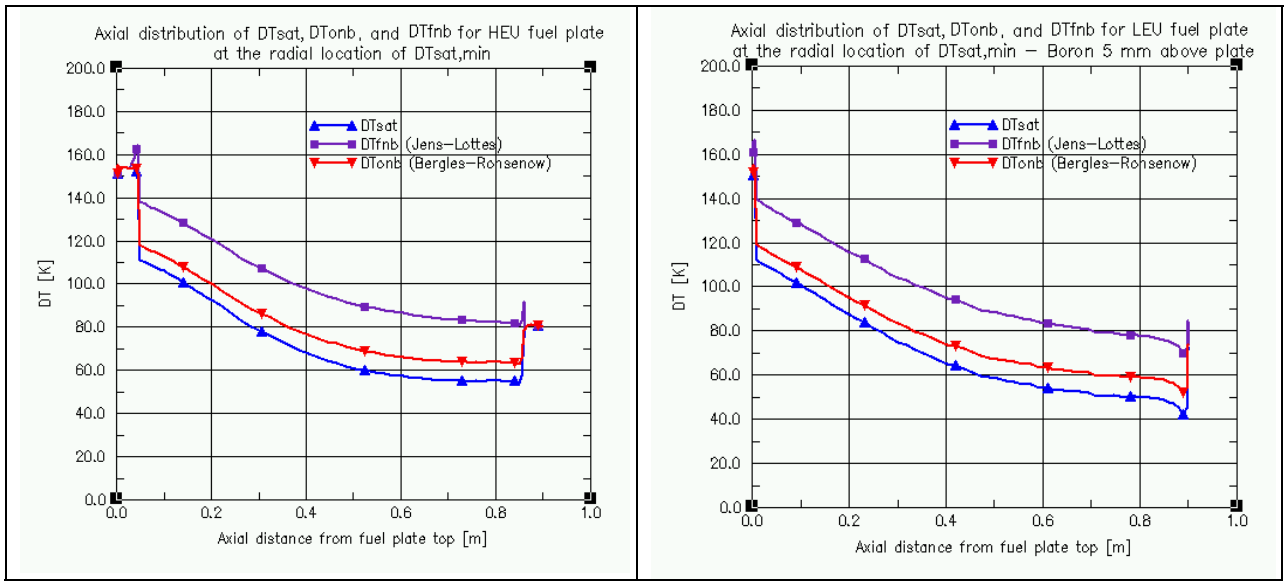

Figure 10: Axial distribution of DTsat, DTonb, and DTfnb:
a) Left, HEU fuel plate, and b) Right, LEU fuel plate

The minimum margins to saturation, FNB and ONB for the HEU and LEU fuel plates are summarized in Table 2. The margins to both ONB and FNB for LEU are lower by approximately 10 K than the same margins for the HEU fuel, when using either the Bergles-Rohsenow correlation or the Jens-Lottes correlation. The minimum value for DTsat and DTonb occurs for the LEU fuel at z = - 0.890 m from the top of the fuel plate (i.e. at the bottom of the fuel meat region), at the radial location R = 191.75 mm. For the HEU fuel plate the minimum margins occur at z = -0.850 m from the top of the fuel plate (i.e. at the bottom of the fuel meat region), at the radial location R = 191.75 mm.

Table 2: Minimum margins to saturation, ONB and FNB for the HEU and LEU nominal cases

	HEU	LEU
DTsat [K]	54.2	42.2
DTonb (Bergles-Rohsenow) [K]	62.7	52.0
DTfnb (Jens-Lottes) [K]	79.4	70.3

The lower margins to saturation, ONB, and FNB for the LEU fuel plate are due in part to the higher neutronic flux at the bottom of the fuel meat as shown in Figure 6 and in part to the lower local coolant pressure, since the fuel meat region extends further down and is closer to the expansion at the entrance to the lower plenum than in the case of the HEU fuel plate. However, the LEU fuel plate maintains a substantial margin to ONB, 52.0 K according to the Bergles-Rohsenow correlation.

It is noted that although in the nominal case studied the minimum margin to ONB occurs at the bottom of the fuel meat region, this location depends on the characteristics of the case analyzed. In the nominal case the coolant flow rate is sufficiently high so that the pressure drop

dominates the axial power generation decrease towards the bottom of the plate. In a case with a lower flow rate however, the pressure gradient is lower and the axial power profile can become dominant, causing the location of the minimum margin to ONB to move up towards the center of the fuel plate where the heat flux and wall-surface temperature are higher.

Following a procedure used in previous RHF safety studies at ILL, we performed a series of HEU and LEU analyses, increasing gradually the power of the reactor in order to determine the power level at which the margin to saturation, ONB, and FNB become zero. The core power levels at which the saturation, ONB, and FNB margins become zero for the HEU and LEU fuel plates are summarized in Table 3.

Table 3: RHF core power levels at which the margins to saturation, ONB, and FNB become zero

	HEU	LEU
P (DTsat = 0) [MW]	95.43	88.65
P (DTonb, br = 0) [MW]	104.54	99.11
P (DTfnb, jl = 0) [MW]	122.23	110.12

Following the ILL approach as described in the SAR [Ref. 5], we have used the power levels in Table 3 to evaluate the margin relative to Vr, the power level at which a scram is initiated. The margin relative to Vr is calculated as:

$$M(V_r) = 100\frac{(0.95P_{boiling} - V_r)}{V_r} \qquad (8)$$

where:

P(boiling) = power level at which the saturation, ONB, or FNB margin becomes zero [MW] (the factor 0.95 takes into account the global power uncertainty)
Vr = 64.13 MW = power level at which scram is initiated for LEU and HEU
M(Vr) = margin relative to Vr, [%]

The margins relative to Vr for the HEU and LEU fuel configurations are summarized in Table 4. The LEU margin to ONB based on the Bergles-Rohsenow correlation is 46.7%. This value is 8.1% lower than the corresponding HEU margin to ONB, but indicates that a substantial margin to ONB exists for the nominal LEU RHF case analyzed.

Table 4: Margin to Saturation, ONB, and FNB relative to Scram Power, Vr, in%

	HEU	LEU
M(Vr) (DTsat = 0) [%]	41.3	31.2
M(Vr) (DTonb, br = 0) [%]	54.8	46.7
M(Vr) (DTonb, jl = 0) [%]	81.0	71.0

Conclusions

A model of the recommended LEU Relocated Poison Configuration fuel plate was developed and analyses of the RHF thermal-hydraulic characteristics were performed for nominal operating conditions. The maximum cladding surface temperature and the margins to saturation, ONB, and FNB for the LEU fuel were determined and compared with the corresponding values for the HEU fuel plate. The results show that the LEU margin to ONB, relative to the scram power level Vr, is approximately 8% lower than the corresponding margin for HEU fuel plate but remains still high at 46.7%, indicating that a substantial margin to ONB exists for the recommended LEU Relocated Poison Configuration analyzed.

Small differences exist between the results obtained with STAR-CD model and those obtained with the CFX model as shown in Table 1. Because the above margin analyses are based on the more conservative results predicted by the STAR-CD model, and based on recent results obtained with an involute-based STAR-CD model that predicts a decrease in the maximum coolant wall-surface temperature of approximately 5 K, we are confident that improved CFD models together with a better understanding of the modeling differences will lead to somewhat lower coolant wall-surface temperatures than those used in the above boiling margin analysis. Therefore, the HEU and LEU margins to coolant boiling shown in Table 4 are likely to increase.

References

[1] A. BERGERON “Conversion of RHF to a low enriched uranium fuel – Neutronic calculations with VESTA”, IRSN report DSU/SEC/T/2009-346

[2] Y. CALZAVARA, S. FUARD “Evaluation of measurements performed on the French high flux reactor (RHF)”, RHF-HWR-RESR-001 CRIT, International Handbook of Evaluated Reactor Physics Benchmark Experiments, Nuclear Energy Agency (OECD), 2009.

[3] STAR-CD Version 3.20 Methodology Manual, CD-adapco, UK (2004)

[4] CFX : http://www.ansys.com/products/fluid-dynamics/cfx/

[5] RHF Safety Analytic Report, released 2004

[6] W. JENS and P. LOTTES, “Analysis of heat transfer, burnout, pressure drop and density data for high-pressure water”, ANL-4267, 1951

[7] A. BERGLES and W. ROHSENOW, "The Determination of Forced-Convection Surface-Boiling Heat Transfer", Journal of Heat Transfer, August 1964